International Journal of Optics and Applications 2015, 5(3): 51-57
DOI: 10.5923/j.optics.20150503.01

SNR and BER Performance Enhancement on FSO Induced by Atmospheric Turbulence Using Optical Spatial Filter

Ucuk Darusalam*, Purnomo Sidi Priambodo, Eko Tjipto Rahardjo

Department of Electrical Engineering, Faculty of Engineering, Universitas Indonesia, Jl. Kampus Baru UI, Depok

Abstract In order to enhance signal-to-noise ratio (SNR) and bit-error-rate (BER) performance on free-space optical (FSO) communications, an optical spatial filter (OSF) is implemented at focus spot of receiver lens. Conceptually, the OSF collects fluctuation of signal intensity that is caused by beam wander and spatial noise at focus spot within a narrow region. The confinement of signal intensity fluctuation in a narrow region that goes random arround the optical axis can minimizes reception of noise into photodetector (PD). It also brings an advantage for enhancing mean value of signal intensity. Hence, PD receives optimum signal power and noise can be minimized. Those noise suppression leads to enhancement SNR performance. It means the distribution of signal power is optimally produced by PD rather than noise. Hence, higher signal intensity and narrow noise bandwidth by the OSF minimize the error distribution that gives an advantage to decrease the order of BER. From the calculations and experiment show that the OSF enhances SNR and BER performance under influenced of turbulence media. In comparison to direct detection (DD) method, the OSF with pinhole of 20 μm and cone reflector of 1.5 mm produces best performance that ⟨SNR⟩ increases at 4.2 dB and ⟨BER⟩ decreases at 10^{-12}.

Keywords FSO, Atmospheric turbulence, Spatial noise, Beam wander, Spatial filter, Cone reflector, Pinhole

1. Introduction

FSO is a potential telecommunication platform that has achieved tremendous development on bit rate capacity, link distance, and integrated in multi-system [1-6]. It has attractive benefit such as free-licensed, low-cost, high-security, and high rate transmission [7]. It has major drawbacks that the SNR and BER performance is strongly influenced by noise modulation of atmospheric turbulence [8]. Some impacts as the results of atmospheric turbulence modulation on optical propagation are beam wander and spatial noise effects [9]. Those lead to fluctuation of amplitude and phase in optical propagation. Those also increase to scale-up with propagation path length and turbulence level on the atmosphere. Through these, signal intensity goes to fluctuation on focus spot of receiver lens randomly. Unfortunately, PD receives those impact in the form of fading, large noise bandwidth, and misalignment detection. It produces lower signal power which frequently falls below a the prescribed threshold level P_{Th} of PD and maximum noise as well. These lead to degradation of SNR. Hence, the lower SNR contributes to higher order of BER. Moreover, SNR and BER performance degrades in maximum by the presence of turbulence effects.

Recently, several methods have been developed to enhance SNR and BER performance on FSO under influenced of atmospheric turbulence. Spatial-diversity (SD), time-diversity (TD), cooperative-diversity (CD), photon detection technique (PDT), amplification method, and adaptive optics (AO) have been investigated so far in order to solve turbulence effects intensively [10-15]. Those methods pay great concern to minimize degradation SNR and BER performance. Generally, those aforementioned methods implement DD for retrieving a signal without an optical treatment previously in a receiver plane. Contrary to the benefit of FSO that has low-cost implementation, those aforementioned methods are quite complex and high-cost. SD offers enhancement SNR and BER performance with multiple system of transmitter and receiver that requires complex electronics of equal gain combiner [10]. TD provides method of signal transmission in multi-periode of time that also requires complex signal processing in the receiver system [11]. CD offers smart combination of spatial- and time-diversity that also requires complex algorythm as well [12]. PDT offers higher sensitivity for lower signal while noise does not taken into account to be suppressed optically [13]. Optical amplification that uses erbium-doped fiber amplifier commonly, also does not provide optical method to enhance signal intensity with

* Corresponding author:
ucuk.darusalam@gmail.com (Ucuk Darusalam)
Published online at http://journal.sapub.org/optics

minimum noise [14]. Moreover, AO offers enhancement of signal intensity with processing of optical propagation technique but beam wander does not taken into consideration as the serious problem to be suppressed [15]. By taking into consideration that beam wander and spatial noise effects can be suppressed optically at focus spot of receiver lens, the OSF can be implemented as a detection method before signal is received by PD. Thus, implementation of the OSF for suppressing noise that is caused by turbulence effects is the motivation of this work in order to enhance SNR and BER performance.

In this paper, the OSF is implemented on FSO of full-duplex transmission at wavelength of 1550 nm. It is a simple- and low-cost method for suppression of beam wander and spatial noise effects. It can be integrated with the aforementioned methods such as optical amplification or SD. It also has competitive benefit for bit rate capacity processing in comparison to TD. The characteristics of turbulence effects are random phenomena and independent process as well. Meanwhile, turbulence effects cannot be treated as a separate process in optical propagation. Thus, beam wander and spatial noise effects cannot be solved separately in order to enhance SNR and BER performance. Regarding those, the OSF is designed to suppress beam wander and spatial noise effects simultaneously. The OSF is composed of cone reflector and pinhole [16] that is installed on focus spot of receiver lens before PD. Cone reflector is designed to suppress beam wander that has random angle of focus spot through directed reflectance radially into pinhole diameter [17]. Pinhole is designed to suppress spatial noise through governing Fresnel diffraction on focus spot. Through suppression of beam wander and spatial noise effects simultaneously, fluctuation of signal intensity and noise reception into PD can be minimized. Thus, as the continuation work in [16, 17], SNR and BER performance enhancement using the OSF is reported through calculations ans experiment.

2. Noise Suppression to Enhance SNR and BER Performance Using the OSF

In Fig. 1, conceptually, the OSF [16, 17] has benefit among ideal of aperture averaging [18] and DD [19]. Technically, ideal of aperture averaging receives incident of optical propagation on receiver lens through multiple reception where $W_{-1} \cong D_G$. Statistically, it produces narrowest noise bandwidth with highest probability of signal intensity. DD that has a requirement for lower diameter of receiver lens than incident of optical propagation where $W_{-1} \gg D_G$ produces wider noise bandwidth and lower probability of mean irradiance. In comparison to DD, the OSF that has reception of optical propagation $W_{-1} \gg D_G$ also through suppression of beam wander and spatial noise effects produces competitive probability of signal intensity with minimum noise bandwidth. However in comparison to ideal of aperture averaging, the OSF has some advantages that are simplicity for reception of optical propagation as in DD, competitive probability of signal intensity, and narrow noise bandwidth.

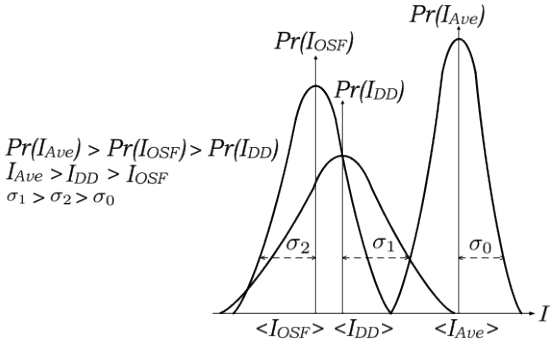

Figure 1. The probability of mean irradiance and noise bandwidth for ideal of aperture averaging Pr (I_{Ave}), direct detection Pr (I_{DD}), and the OSF Pr (I_{OSF}) on FSO

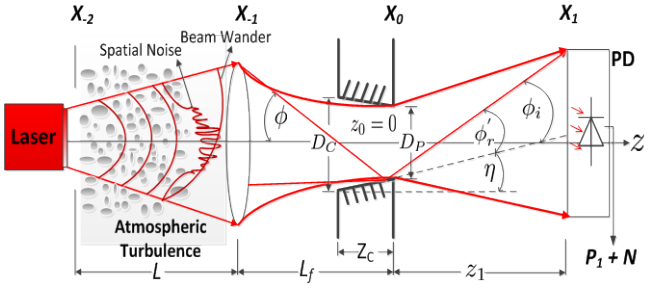

Figure 2. The optical system for suppression of beam wander and spatial noise effects in FSO under atmospheric turbulence. It is composed of a transmitter plane $\boldsymbol{X_{-2}}$, a receiver lens plane $\boldsymbol{X_{-1}}$, the OSF plane $\boldsymbol{X_0}$, PD plane $\boldsymbol{X_1}$, and $\boldsymbol{z_0 = 0}$ is the origin where optical propagation from laser source directs from $\boldsymbol{X_{-2}}$ into $\boldsymbol{X_{-1}}$ [17]

In Fig. 2, The incident of optical propagation that modulates noise on receiver lens X_{-1} is focused onto pinhole radius Δr_0 of X_0. Focus spot that coincidence on X_0 goes fading where fluctuation of signal intensity goes higher and falls below P_{Th}. Unfortunately, beam wander also leads misdetection into PD frequently. In order to suppress noise, The OSF governs Fresnel diffraction and reflectance of beam wander on focus spot before PD. The mean of signal intensity as the output of the OSF at X_1 under atmospheric turbulence is given below [17],

$$\langle I_1(\boldsymbol{r_1}, z_1 \approx 0, \phi_i)\rangle = \frac{1}{4} I_{-1}^0(0, -L_f)\frac{W_G^2}{W_0^2}\, SR \exp\left(-SR\frac{2(\Delta r_0)^2}{W_0^2}\right)\cos(\phi_i) \times [1 - 2\cos(v)\ J_0(v) + J_0^2(v)], \quad (1)$$

where brackets $\langle . \rangle$ denotes mean value. In Eq. (1), $\boldsymbol{r_0}$, W_G, W_0, ϕ_i, J_0, $I_{-1}^0(0, -L_f) = W_{-2}^2/W_{-1}^2$, $\Lambda_{-1} = 2L/kW_{-1}^2$, $SR = 1/\left(1 + 1.63\,\sigma_R^{12/5}(L)\,\Lambda_{-1}\right)$, $v = [2\pi\Delta r_0/\lambda z_1]r_1$, $\sigma_R^{12/5}(L) = \left(1.23\,C_n^2\,k^{7/6}\,L^{11/6}\right)^{6/5}$, and $k = 2\pi/\lambda$ are radius coordinate at $\boldsymbol{X_0}$, the effective aperture radius of receiver lens on $\boldsymbol{X_{-1}}$, focus spot radius, reflectance beam wander angle from cone reflector into pinhole diameter with respect to optical axiz Z as shown in Fig. 2, Bessel function of the first kind, free-space irradiance of optical propagation

that incident on receiver lens of $\boldsymbol{X_{-1}}$, the effective of optical propagation that incident on receiver lens for path length L, Sthrel ratio, spatial frequency at radius $\boldsymbol{r_1}$ on $\boldsymbol{X_{-1}}$ as the function of spacing distance z_1, Rytov variance for propagation path length L, and wave number, respectively.

In Eq. (1), ϕ_i that is reflectance angle from cone reflector for incident beam wander angle ϕ has a range of ϕ_{min} to ϕ_{max} as stated below [17],

$$\phi_i = \phi_r^{'} + \eta = \phi + 2\eta = \phi + 2\tan^{-1}\left(\frac{D_C - D_P}{2Z_C}\right), \quad (2)$$

$$\phi_{min} = \phi^0 + \tan^{-1}\left(\frac{\frac{1}{2}(D_G - D_P)}{L_f}\right), \quad (3)$$

$$\phi_{max} = \phi_{min} + \tan^{-1}\left(\frac{\frac{1}{2}(D_G - D_C)}{L_f - Z_C}\right), \quad (4)$$

where ϕ^0, D_G, D_P, Z_C, η, $\phi_r^{'}$, and L_f are maximum angle of focus spot from receiver lens of $\boldsymbol{X_{-1}}$ that incident at $\boldsymbol{X_0}$ for condition of non-turbulent atmosphere, hard diameter of receiver lens, pinhole diameter, tilt angle of cone reflector, reflectance angle with respect to tilt plane of cone reflector, and length of focus spot, respectively.

Turbulence effects that arise in optical propagation lead to fluctuation of signal intensity and maximum noise modulation. As shown in Eq. (1), Sthrel ratio characterizes beam wander and spatial noise on incident of optical propagation W_{-1}. Beam wander that arises also causes beam spreading where focus spot W_0 moves wider arround the optical axis Z randomly. Hence, focus spot experiences long-term beam spreading. Meanwhile, short-term beam spreading or spatial noise also arises as well. The signal intensity in focus spot goes lower as stated in Eq. (1) by term of $I_{-1}^0(0, -L_f)(W_G^2/W_0^2)SR$. It means signal intensity goes fading where fluctuates randomly by the presence of beam wander and spatial noise. Hence, PD produces minimum of signal power and maximum noise. The OSF which consists of pinhole with radius of $0 \le \Delta r_0 \le D_P/2$ governs diffraction at $\boldsymbol{X_0}$. As shown by Eq. (1), pinhole produces near-field distribution of Fresnel diffraction at $z_1 \approx 0$ of $\boldsymbol{X_1}$. By those mechanism, signal intensity $\langle I_1(\boldsymbol{r_0}, z_1 \approx 0, \phi_i)\rangle$ from pinhole is minimum of noise modulation.

By suppression of beam wander and spatial noise effects on focus spot, PD receives fundamental component of diffraction in optimum since $z_1 \approx z_0$ and $\boldsymbol{r_0} \approx \boldsymbol{r_1}$. It produces the mean of signal power $\langle P_1\rangle$ as stated below [17],

$$\langle P_1(\boldsymbol{r_1}, z_1 \approx 0, \phi_i)\rangle = \frac{\pi}{2}\frac{W_G^2}{W_0^2} I_{-1}^0(0, -L_f)\, SR\, \exp\left(-SR\frac{2(\Delta r_0)^2}{W_0^2}\right)\cos(\phi_i)\, B, \quad (5)$$

where B is the circular aperture function of pinhole that is given below [17],

$$B = \frac{r_1^2}{2} - \left[\frac{2A^2 r_1^2}{3}\cos(Ar_1)\, J_0(Ar_1) + \frac{A^2 r_1^2 \sin(Ar_1) - Ar_1\cos(Ar_1)}{3} J_1(Ar_1)\right] + \left[\frac{A^2 r_1^2}{2}\left(J_0^2(Ar_1) + J_1^2(Ar_1)\right)\right], \quad (6)$$

where $A = [2\pi\Delta r_0/\lambda z_1]$ and J_1 is Bessel function of second kind. In comparison to DD [18, p.459], $\langle P_1\rangle$ in Eq. (5) is increased by term of $I_1(\boldsymbol{r_1}, z_1 \approx 0, \phi_i)$. The mean of signal power from the OSF is produced higher by PD. Term of B in Eq. (5) works in optimum for noise suppression where $z_1 \approx 0$. Term of $\cos(\phi_i)$ in Eq. (5) also provides suppression of beam wander in order to minimize misalignment detection that is caused by random displacement of focus spot. It means, the OSF suppresses beam wander and spatial noise effects simultaneously. Thus, PD produces optimum of signal power with minimum noise.

Regarding enhancement of received signal power $\langle P_1\rangle$ by PD in Eq. (5) as the compensation for confinement of signal intensity fluctuation in narrow region of pinhole through reflectance of cone reflector, $\langle SNR\rangle$ degradation can be minimized by the OSF. $\langle SNR\rangle$ is increased by suppression of signal power ratio, $P_1^0/\langle P_1\rangle$. The OSF minimizes those ratio in order to enhance $\langle SNR\rangle$ as given below [20],

$$\langle SNR\rangle = \frac{SNR^0}{\left(\frac{P_1^0}{\langle P_1\rangle} + \sigma_I^2(D_G)(SNR^0)^2\right)^{\frac{1}{2}}}, \quad (7)$$

where SNR^0 and P_1^0 are optimum value of SNR and signal power P_1 in the absence of atmospheric turbulence, respectively. In Eq. (7), the irradiance flux variance $\sigma_I^2(D_G)$ has range value of 0-1 for weak to strong turbulence level. Frequently, signal power P_1 falls below P_{Th}. The OSF enhances value of $\langle I_1(\boldsymbol{r_1}, z_1 \approx 0, \phi_i)\rangle$. Thus PD produces signal power P_1 beyond P_{Th}. Signal power ratio $P_1^0/\langle P_1\rangle$ is decreased by the OSF as stated below,

$$\frac{P_1^0(\boldsymbol{r_1}, z_1 \approx 0)}{\langle P_1(\boldsymbol{r_1}, z_1 \approx 0, \phi_i)\rangle} = \frac{W_0^2}{SR\, \exp\left(-SR\frac{2(\Delta r_0)^2}{W_0^2}\right)\cos(\phi_i)\, B}. \quad (8)$$

The optimum suppression of $P_1^0/\langle P_1\rangle$ produces $\langle SNR\rangle$ that approximate to SNR^0. In comparison to DD that $P_1^0/\langle P_1\rangle \cong 1/SR$ [18, p. 460], this ratio is decreased into minimum value by the OSF as shown in Eq. (8). Thus, the OSF gives advantage to minimize signal power ratio $P_1^0/\langle P_1\rangle$ by suppressing beam wander and spatial noise effects simultaneously.

Generally, probability density function uses gamma-gamma distribution $p_I(u)$ as the channel model for FSO at atmospheric turbulence [18, p. 462]. $p_I(u)$ is the probability of signal unit $u = S/i_S$ that is influenced by α and β as the representations of small- and large-scale of atmospheric turbulence, respectively. $\langle SNR\rangle$ enhancement by the OSF minimizes the probability of $\langle BER\rangle$. Based on [20], $\langle BER\rangle$ can be suppressed into lower order through $\langle SNR\rangle$ enhancement. Furthermore, $\langle BER\rangle$ of OOK modulation method is derived from [20] with regards to integral solution in [21]. $\langle BER\rangle$ is stated below,

$$\langle BER\rangle = \frac{1}{4}p_I^2(u)\, erfc\left(\frac{\langle SNR\rangle u}{2\sqrt{2}}\right) + \frac{1}{\langle SNR\rangle^2}\, erf\left(\frac{\langle SNR\rangle u}{2\sqrt{2}}\right) - \frac{u\sqrt{2}}{\langle SNR\rangle 2\sqrt{\pi}}\, exp\left(-\frac{\langle SNR\rangle^2 u^2}{8}\right). \quad (9)$$

$\langle BER\rangle$ in Eq. (9) is determined by $\langle SNR\rangle$ and $p_I(u)$. In order to achieve lower order of $\langle BER\rangle$ under turbulence

effects, $\langle SNR \rangle$ must be increased higher. Since the OSF suppresses noise, signal intensity $\langle I_1(\boldsymbol{r_1}, z_1 \approx 0, \phi_i) \rangle$ increases higher than in DD. Hence, PD produces optimum of signal power $\langle P_1 \rangle$ rather than noise. It means the OSF decreases the signal power ratio of $P_1^0/\langle P_1 \rangle$ in order to enhance $\langle SNR \rangle$. Furthermore, by the improvement of $\langle SNR \rangle$, $\langle BER \rangle$ also decreases into lower order as well. In comparison to DD, $\langle BER \rangle$ is produced lower by the OSF, since $\langle SNR \rangle$ is increased by suppression of $P_1^0/\langle P_1 \rangle$ as stated in Eq. (8).

3. Experimental Set-up

In Fig. 3, the experiment of FSO with full-duplex transmission implement wavelength, λ of 1.55 μm. Bit rate transmission of 1 Gbps with OOK modulation is also used. Optical propagations are separated into box of turbulence simulator (BTS). For reference, optical propagation of backward-directed from beam collimator BC-1 into receiver lens-1 is conditioned with non-turbulent media. Optical propagation of forward-directed of from beam collimator BC-2 into receiver lens-2 is induced by turbulence media in BTS. The properties of optical propagation are W_{-2} of 0.015 m, W_{-1} of 0.15 m, and W_0 of 500.0 μm. P_{-2}^0 of +16.5 dBm is transmitted out from BC-2 into receiver lens-2. The properties of receiver lens are D_G of 0.05 m and L_f of 0.1 m. P_{Th} of −25.0 dBm is P_{Th} for PD-1 and PD-2. The optical power meter (OPM) and BER tester are used on experiment for SNR and BER measurements, respectively.

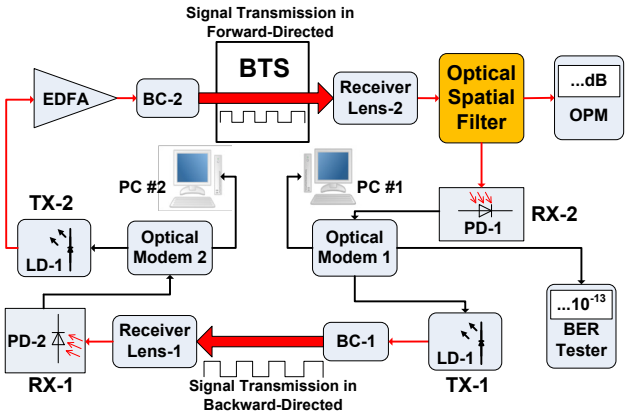

Figure 3. FSO of full-duplex transmission using wavelength of 1.55 μm that transmitting 1 Gbps of data rate on turbulence media of BTS while for measurement of performance, OPM (Optical Power Meter) and BER tester are used

In Fig. 4, BTS that provides turbulence media is designed for optical propagation of forward-directed in order to achieve beam wander and spatial noise modulation randomly.

For constant parameters of cone reflector $D_C = 1.5\ mm$ and $Z_C = 2.0\ mm$, the OSF is designed with various pinhole diameter that are 50.0 μm, 40.0 μm, 30.0 μm, and 20.0 μm for D_{P1}, D_{P2}, D_{P3}, and D_{P4}, respectively. Based on Eqs. (3) and (4) for $\phi^0 = 14^o$ and both contant values D_C and Z_C, the range of beam wander ϕ that can be received by cone reflector is $\phi_{min} = 28^o$ to $\phi_{max} = 38^o$. In order to produce optimum reflection at 1.55 μm, the OSF is made from material of silver [22]. Furthermore, in order to achieve Fresnel diffraction, the OSF is installed on focus spot of receiver lens where pinhole is at $z = 0$ on $\boldsymbol{X_0}$ and PD is placed on $\boldsymbol{X_1}$ near to pinhole output of the OSF where spacing distance z_1 is at the order of $10^{-4}\ m$.

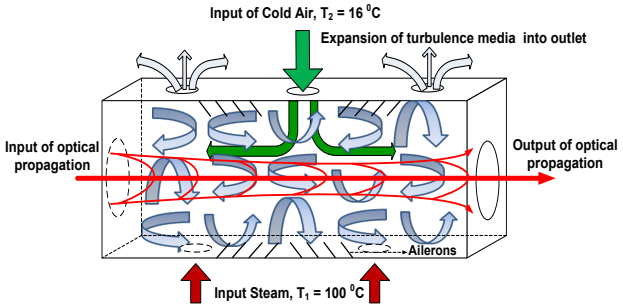

Figure 4. Box of turbulence simulator (BTS) providing turbulence media to induce optical propagation of forward-directed. BTS is designed for volume dimension of 4.0 $m \times 0.5\ m \times 0.5\ m$ where turbulence media is constituted by the mixing flows of high temperature-gradient. The steam at T of $100^o C$ with low-speed and cold air at T of $16^o C$ with wind-speed of 8.0 m/s are flowed altogether along the BTS volume. Furthermore, the flows are broken-up by ailerons that is installed along the path length inside BTS [17]

4. Results and Discussion

The calculations of $\langle SNR \rangle$ and $\langle BER \rangle$ for DD and the OSF are shown in Figs. 6 and 7. $SNR^0 = 40.0\ dB$ is chosen as reference for analysis. The calculations are based on values of index structure, $C_n^2 = 5 \times 10^{-13} m^{-2/3}$. The properties of optical propagation are set based on the experiment. Based on the ϕ^0, ϕ_{min}, and ϕ_{max} that are stated in Eqs. (3) and (4), $\phi_1 = 18^o$, $\phi_2 = 28^o$, and $\phi_3 = 38^o$ are chosen as beam wander angles. $\alpha = 3$ and $\beta = 2$ are set constant for calculations. α is chosen higher than β, since it is dominant factor for SNR and BER performance degradation under atmospheric turbulence.

In Figs. 5 and 6, the performance of DD degrades in maximum by the presence of beam wander and spatial noise effects where $\langle SNR \rangle = 34.4\ dB$ and $\langle BER \rangle = 10^{-4}$. The OSF improves $\langle SNR \rangle$ degradation that presents in DD. $\langle SNR \rangle$ increases linear as D_P of the OSF goes lower for beam wander angles of ϕ_1, ϕ_2, and ϕ_3. The performance of FSO for ϕ_1 is better than at ϕ_2 and ϕ_3. Beam wander angle ϕ_1 is at the range that is received by pinhole directly without reflectance of cone reflector. The range of beam wander angle for direct reception by pinhole is $14^o - 27^o$. While range of beam wander angle for reflectance by cone reflector is $28^o - 38^o$. However, for ϕ_2 and ϕ_3 SNR and BER performance is achieved better than DD. Recalled Eq. (8), $P_1^0/\langle P_1 \rangle$ determines value of $\langle SNR \rangle$. Thus, the OSF produces lower value of $P_1^0/\langle P_1 \rangle$ for lower D_P. $\langle SNR \rangle$ performance for the OSF is better than DD since D_P goes lower as well. The OSF improves $\langle SNR \rangle$ through suppression of beam wander and spatial noise effects

simultaneously. It governs Fresnel diffraction as can be seen by the circular aperture function of pinhole B that is stated in Eq. (6). Hence the OSF minimizes $P_1^0/\langle P_1\rangle$ since D_P goes lower. Even for larger pinhole diameter D_{P1}, $\langle SNR\rangle$ is produced higher by the OSF than DD for ϕ_1, ϕ_2, and ϕ_3. The OSF also improves $\langle BER\rangle$ degradation as D_P goes lower as well. It produces higher $\langle SNR\rangle$ in order to achieve lower order of $\langle BER\rangle$ for ϕ_1, ϕ_2, and ϕ_3 as well. Suppression of beam wander and spatial noise effects by the OSF is achieved through minimizing signal power ratio $P_1^0/\langle P_1\rangle$ as shown by Eq. (8).

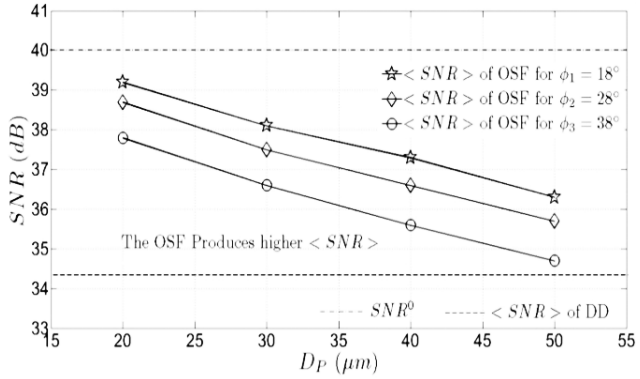

Figure 5. The calculation results where $\langle SNR\rangle$ vs. D_P is from the OSF for $\phi_1 = 18^o$, $\phi_2 = 28^o$, and $\phi_3 = 38^o$, $\langle SNR\rangle = 34.4\ dB$ is from DD and $SNR^0 = 40.0\ dB$

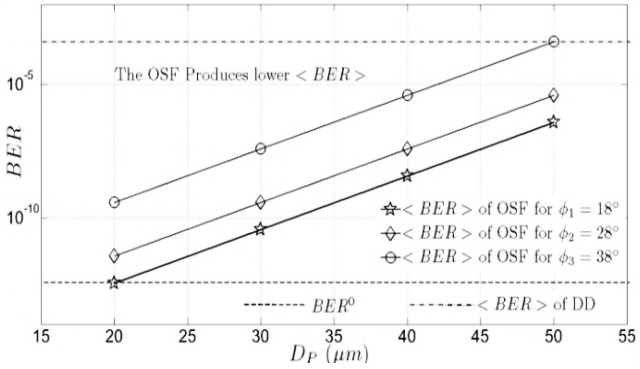

Figure 6. The calculation results where $\langle BER\rangle$ vs. D_P is from the OSF method for $\phi_1 = 18^o$, $\phi_2 = 28^o$, and $\phi_3 = 38^o$, $\langle BER\rangle = 10^{-4}$ is from DD, and $BER^0 = 10^{-13}$

In Fig. 7, experiment results of $\langle SNR\rangle$ vs. D_P for DD and the OSF are shown. $\langle SNR\rangle$ of DD is 34.9 dB. Regarding $SNR^0 = 40.0\ dB$, this performance quite degrades by the presence of beam wander and spatial noise modulation that arise randomly in BTS. The OSF improves those degradation in scale of 2.5 dB, 3.5 dB, 3.8 dB, and 4.2 dB for D_{P1}, D_{P2}, D_{P3}, and D_{P4}, respectively. $\langle SNR\rangle$ improvement by the OSF is better than DD. But $\langle SNR\rangle$ improvement by different of D_P do not contribute to higher value. The OSF for each of D_P tend to produce the same value of $\langle SNR\rangle$. For example, D_{P2} and D_{P3} do not produce high different value of $\langle SNR\rangle$. Only D_{P4} produces highest $\langle SNR\rangle$ that approximates SNR^0. However, the experiment result in Fig. 8 shows the same trend as the calculation in Fig. 6, that $\langle SNR\rangle$ is increased by the OSF since D_P goes lower.

In Fig. 8, experiment results of $\langle BER\rangle$ vs. D_P for DD and the OSF method are shown. $\langle BER\rangle$ of DD is produced at 1.9×10^{-5}. Regarding $BER = 1.0\times10^{-13}$ at SNR^0, those performance quite degrades also. The OSF improves $\langle BER\rangle$ degradation in scale of 10^{-2}, 10^{-4}, 10^{-6}, and 10^{-7} for D_{P1}, D_{P2}, D_{P3}, and D_{P4}, respectively. $\langle BER\rangle$ improvements by different of D_P are significant. They achieve in scale range of 10^{-1} to 10^{-5} for D_{P1} to D_{P4}. D_{P4} produces $\langle BER\rangle$ that approximate to BER at SNR^0. Moreover, Fig. 8 shows the same trend as Fig. 7, that $\langle BER\rangle$ is decreased to lower order by the OSF since D_P goes lower as well.

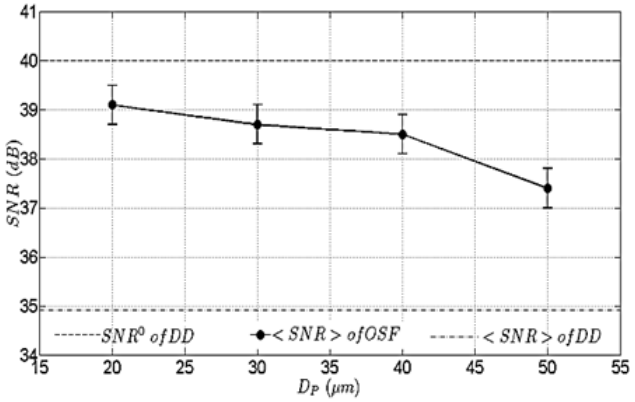

Figure 7. The experiment results where $\langle SNR\rangle$ vs. D_P from the OSF, $\langle SNR\rangle = 34.9\ dB$ is from DD, and $SNR^0 = 40.0\ dB$

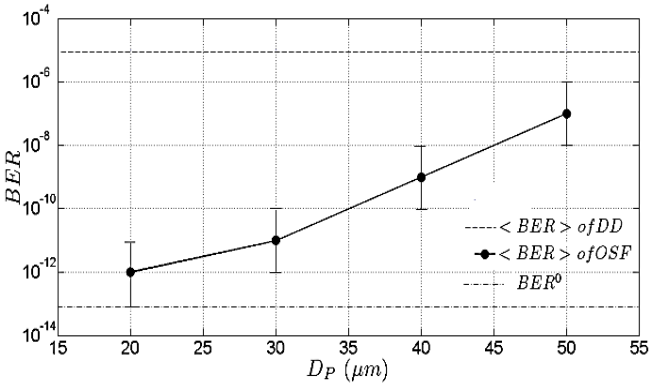

Figure 8. The experiment results where $\langle BER\rangle$ vs. D_P is from the OSF, $\langle BER\rangle = 10^{-5}$ is from DD, and $BER^0 = 10^{-13}$

For long propagation path where beam wander and spatial noise are modulated higherly, the OSF is a potential detection method on FSO to overcome fading, noise, and misalignment of detection undergo randomly. In order to suppress noise optimally for long propagation path, the circular aperture function B can be optimized by considering the ratio of pinhole diameter and spacing distance between the OSF and PD. Thus, term of $\cos(v)$ in Eq. (2), $v = [2\pi\Delta r_0/\lambda z_1]r_1 \approx 0$ leads to $(D_P/2) = \lambda z_1/4r_1$. Furthermore, for larger beam wander angle ϕ, the tilt angle of cone reflector η also has significant contribution to reflect random displacement of focus spot. In order to fullfill this, parameters for cone reflector must consider term of $2\ tan^{-1}(D_C - D_P/2Z_C)$ of Eq. (2). Thus,

maximum tilt angle of cone reflector is $tan^{-1}(D_C - D_P/2Z_C) < \phi$. Hence, wider range of ϕ_{min} to ϕ_{max} can be received by cone reflector largely. By considering those aforementioned conditions, the OSF brings some advantages such as noise suppression in optimum and fading in minimum. Moreover, misalignment of detection that is caused by larger beam wander angle can be minimized by cone reflector as well.

5. Conclusions

The OSF enhances SNR and BER performance on FSO as shown by results of calculation and experiment. In comparison to DD, SNR and BER performance by the OSF is produced better. Based on both calculations and experiment, $\langle SNR \rangle$ increases higher and $\langle BER \rangle$ also decreases to lower order as pinhole diameter of the OSF goes lower. From the calculations, the range of beam wander angle that can be received by cone reflector of the OSF is $28^o - 38^o$ while for $14^o - 27^o$ is received by pinhole directly without reflectance. Thus, the OSF receives beam wander angle in the range of $14^o - 38^o$. From the experiment, $\langle SNR \rangle$ increases from 2.5 to 4.2 dB and $\langle BER \rangle$ decreases from 10^{-7} to 10^{-12}. The OSF suppresses noise in narrow area for minimizing fluctuation of signal intensity. Thus, PD produces optimum of signal power and minimum noise.

ACKNOWLEDGEMENTS

The authors acknowledge Mr. Surma in Opto-Electrotechnique and Laser Application of Universitas Indonesia for his contribution in Lab. facilities.

REFERENCES

[1] V. W. S. Chan, "Free-space optical communications," *J. Lightw. Technol.*, vol. 24, pp. 4750–4762, (2006).

[2] K. Wakamori, K. Kazaura, and Ikuo Oka, "Experiment on regional broadband network using free-space-optical communication systems," *J. Lightw. Technol.*, vol. 25, pp. 3265–3273, (2007).

[3] F. Li, Z. Cao, X. Li, Ze Dong, and L. Chen, "Fiber-wireless transmission system of DM-MIMO-OFDM at 100 GHz frequency," *J. Lightw. Technol.*, vol. 31, pp. 2394–2399, (2013).

[4] R. Paudel, Z. Ghassemlooy, H. Le-Minh, S. Rajbhandari, "Modelling of free space optical link for ground-to-train communications using a Gaussian source," *IET Optoelectron.*, vol. 7, pp. 1–8, (2013).

[5] E. Ciaramella, Y. Arimoto, G. Contestabile, M. Presi, A. D'Errico, V. Guarino, and M. Matsumoto, "1.28 Terabit/s (3240 Gbit/s) WDM transmission system for free space optical communications," *IEEE J. Sel. Areas Commun.*, vol. 27, pp. 1639–1645, (2009).

[6] M. Karimi and M. Nasiri-Kenari, "Free space optical communications via optical amplify-and-forward relaying," *J. Lightw. Technol.*, vol. 29, pp. 242–248, (2011).

[7] C. Liu, Y. Yao, J. Tian, Y. Yuan, Y. Zhao, and B. Yu, "Packet error rate analysis of DPIM for free-space optical links with turbulence and pointing errors," *Chin. Opt. Lett.*, 12, S10101, (2014).

[8] C. Liu, Y. Yao, Y. Yang, Y. Yuan, Y. Zhao, and B. Yu, "Performance of free-space optical communication systems using circle polarization shift keying with spatial diversity receivers," *Chin. Opt. Lett.*, 11, S20101, (2013).

[9] C. Si, Y. Zhanga, Y. Wang, J. Wang, and J. Jia, "Average capacity for non-Kolmogorov turbulent slant optical links with beam wander corrected and pointing errors," *J. of Optik*, vol. 123, pp. 1–5, (2012).

[10] M. A. Khalighi, N. Schwartz, N. Aitamer, and S. Bourennane, "Fading reduction by aperture averaging and spatial diversity in optical wireless systems," *IEEE J. Opt. Commun. Netw.,* vol. 1, pp. 580–593, (2011).

[11] J. Cheng, Y. Ai, and Y. Tan, "Improved free space optical communications performance by using time diversity," *Chin. Opt. Lett.*, 6, pp. 797-799, (2008).

[12] C. A. Rjeily and A. Slim, "Cooperative diversity for free-space optical communications: transceiver design and performance analysis," *IEEE Trans. Commun.*, vol. 59, pp. 658–663, (2011).

[13] C. Rivera and M. A´ lvarez, "Assessment of PbSe photoconductors for the realization of free-space mid-infrared optical communication links," *IEEE Photon. Technol. Lett.*, vol. 24, pp. 267–269, (2012).

[14] M. A. Kashani, M. M. Rad, M. Safari, and M. Uysal, "All-optical amplify-and-forward relaying system for atmospheric channels," *IEEE Commun. Lett.*, vol. 16, pp. 1684–1687, (2012).

[15] Y. Yuan, Y. Cai, J. Qu, H. T. Eyyuboglu, and Y. Baykal, "Average intensity and spreading of an elegant Hermite-Gaussian beam in turbulent atmosphere," *Opt. Express,* vol. 17, pp.11130–11139, (2009).

[16] P. S. Priambodo, U. Darusalam, and E. T. Rahardjo, "Free-space optical propagation noise suppression by Fourier optics filter pinhole," *International Journal of Optics and Applications*, vol. 5, pp. 27–32, (2015).

[17] U. Darusalam, P. S. Priambodo, and E. T. Rahardjo, Optical spatial filter for suppression of beam wander and spatial noise effects on FSO induced by atmospheric turbulence, under revision in *Journal of Advances in Optical Technologies*, April, (2015).

[18] L. C. Andrews and R. L. Phillips, *Laser Beam Propagation through Random Media* (Philadelphia, PA: SPIE Press, 2nd ed., (2005).

[19] Z. Zhao, R. Liao, S. D. Lyke, and M. C. Roggemann, "Direct detection free-space optical communications through atmospheric turbulence," IEEEAC #1272, pp. 1–9, (2010).

[20] I. Toseli, L.C. Andrews, R. L. Philips, and V. Ferrero, "Free space optical system performance for a Gaussian beam

propagating through non-Kolmogorov weak turbulence, *IEEE Trans. Antennas Propag.*," vol. 57, pp. 1783–1788, (2009).

[21] E. W. Ng and M. Geller, "A table of integrals of the error functions," *J. of Research of the National Bureau Standard – B. Mathematical Sciences*, 73B, pp. 1–20, (1969).

[22] J. M. Bennett and E. J. Ashley, "Infrared reflectance and emittance of silver and gold evaporated in ultrahigh vacuum," *Appl. Opt.*, vol. 4, pp. 221–224, (1965).